The Astrophysical Journal Letters, 904:L19 (6pp), 2020 December 1 https://doi.org/10.3847/2041-8213/abc6a2

Chandra Observations of the Newly Discovered Magnetar Swift J1818.0–1607

Harsha Blumer[1,2] and Samar Safi-Harb[3]
[1] Department of Physics and Astronomy, West Virginia University, Morgantown, WV 26506, USA; harsha.blumer@mail.wvu.edu
[2] Center for Gravitational Waves and Cosmology, West Virginia University, Chestnut Ridge Research Building, Morgantown, WV 26505, USA
[3] Department of Physics and Astronomy, University of Manitoba, Winnipeg, MB R3T 2N2, Canada; samar.safi-harb@umanitoba.ca
Received 2020 August 26; revised 2020 October 27; accepted 2020 October 31; published 2020 November 26

Abstract

Swift J1818.0–1607 is a new radio-loud magnetar discovered by the Swift Burst Alert Telescope on 2020 March 12. It has a magnetic field $B \sim 2.5 \times 10^{14}$ G, spin-down luminosity $\dot{E} \sim 7.2 \times 10^{35}$ erg s^{-1}, and characteristic age $\tau_c \sim 470$ yr. Here we report on the Chandra observations of Swift J1818.0–1607, which allowed for a high-resolution imaging and spectroscopic study of the magnetar and its environment. The 1–10 keV spectrum of the magnetar is best described by a single blackbody model with a temperature of 1.2 ± 0.1 keV and an unabsorbed flux of $1.9^{+0.4}_{-0.3} \times 10^{-11}$ erg cm^{-2} s^{-1}. This implies an X-ray luminosity of $9.6^{+2.0}_{-1.5} \times 10^{34}\ d_{6.5}^2$ erg s^{-1} and efficiency of $L_X/\dot{E} \sim 0.13\ d_{6.5}^2$ at a distance of 6.5 kpc. The Chandra image also shows faint diffuse emission out to $\geqslant 10''$ from the magnetar, with its spectrum adequately described by a power law with a photon index of 2.0 ± 0.5 and a luminosity of $\sim 8.1 \times 10^{33}\ d_{6.5}^2$ erg s^{-1}. The extended emission is likely dominated by a dust-scattering halo and future observations of the source in quiescence will reveal any underlying compact wind nebula. We conclude that Swift J1818.0–1607 is a transient source showing properties between high-B pulsars and magnetars, and could be powered at least partly by its high spin-down, similar to rotation-powered pulsars.

Unified Astronomy Thesaurus concepts: High energy astrophysics (739)

1. Introduction

Magnetars are young neutron stars with extremely strong magnetic fields (B), often surpassing $\sim 10^{14}$ G, and believed to be powered mainly by magnetic energy dissipation. They emit short ($\sim$0.1 s), bright hard X-ray bursts over the course of days to months, accompanied by changes to their spectral and temporal properties or radio detection (Kaspi & Beloborodov 2017). Several observational results in the last few years have demonstrated that the magnetar family extends beyond the aforementioned canonical observational properties. This includes the discovery of magnetar-like bursts from the rotation-powered pulsars (PSRs) J1846–0258 (Gavriil et al. 2008; Kumar & Safi-Harb 2008) and J1119–6127 (Younes et al. 2016; Göğüş et al. 2016; Archibald et al. 2016), central compact objects (Rea et al. 2016), and low-B magnetars (e.g., Rea et al. 2010). These results present a remarkable set of observational properties of the magnetar population and a testing ground for different emission mechanism models in these sources.

On 2020 March 12, the Swift Burst Alert Telescope (BAT) on board the Neil Gehrels Swift Observatory triggered on a short ($\sim$0.1 s), soft burst indicating the discovery of a new magnetar (Evans et al. 2020) and Swift X-ray Telescope (XRT) observations revealed an uncataloged X-ray source, Swift J1818.0–1607 (hereafter J1818). This was followed by Neutron star Interior Composition Explorer (NICER) observations that led to the detection of a coherent periodicity at 0.733417(4) Hz with significance exceeding 5σ (Enoto et al. 2020). The short burst detected with Swift together with NICER observations suggest that J1818 is a new Galactic magnetar with a spin period of 1.36 s, which is the shortest among the known magnetars, but longer than the period of high-B field rotation-powered pulsars with magnetar-like activity (Enoto et al. 2020).

Radio follow-up observations by the 100 m Effelsberg radio telescope in a band centered on 1.37 GHz identified J1818 as the fifth radio-loud magnetar with a dispersion measure (DM) of 706 ± 4 pc cm^{-3} (Karuppusamy et al. 2020) and provided a first measurement of the spin period derivative of 8.2×10^{-11} s s^{-1} (Champion et al. 2020). Simultaneous observations were performed with X-ray Multi-Mirror Mission (XMM)-Newton and NuSTAR three days after the magnetar burst, where the source spectrum was described by an absorbed blackbody (BB) with interstellar absorption $N_H = (1.22 \pm 0.03) \times 10^{23}$ cm^{-2} and temperature $kT = 1.19 \pm 0.02$ keV plus a power law (PL) with photon index $\Gamma = 0.1 \pm 1.2$ in the 0.3–20 keV energy band (Esposito et al. 2020). The X-ray timing analysis performed with NICER suggested a dipolar magnetic field $B \sim 2.5 \times 10^{14}$ G, spin-down luminosity $\dot{E} \sim 7.2 \times 10^{35}$ erg s^{-1}, and characteristic age $\tau_c \sim 470$ yr (Hu et al. 2020).

We report here on our Chandra Director's Discretionary Time (DDT) observation taking advantage of Chandra's subarcsecond spatial resolution to study J1818 and the effect of magnetar-like outburst on its surrounding.

2. Observation and Data Reduction

The Chandra X-ray Observatory observed J1818 with the Advanced CCD Imaging Spectrometer spectroscopic array (ACIS-S) on 2020 April 3 for an on-source exposure time of 30 ks (ObsID 23209). The source was positioned on the back-illuminated S3 chip and the data were taken in full-frame timed-exposure mode with VFAINT telemetry format. The standard processing of the data was performed using the *chandra_repro* script in CIAO version 4.12[4] (CALDB 4.9.1). The event files were reprocessed (from level 1 to level 2) to remove pixel randomization and to correct for charge-coupled device (CCD) charge transfer efficiencies. An examination of the background light curves did not show any strong flares. The bad grades were filtered out and good time intervals were

[4] http://cxc.harvard.edu/ciao

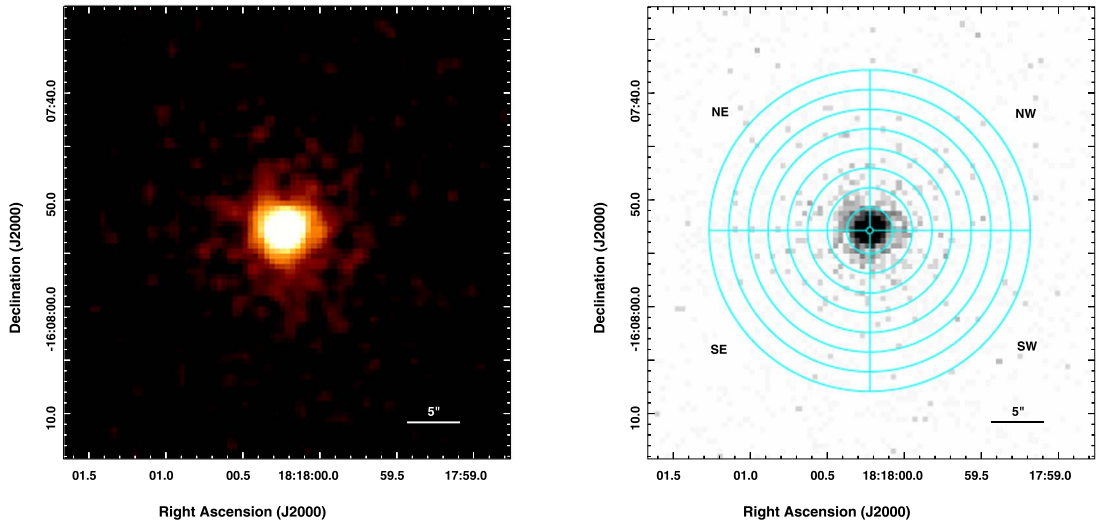

Figure 1. Images of J1818 and surrounding diffuse emission in the 0.5–7 keV energy band. The images are exposure-corrected and shown in logarithmic scale. The smoothed (left panel) and unsmoothed (right panel) images are in units of photons cm^{-2} s^{-1} $arcsec^{-2}$ and counts $pixel^{-1}$, respectively. Overlaid on the unsmoothed image are annular regions divided into four quadrants (shown in cyan), oriented to the north (N), east (E), south (S), and west (W), for radial profile analysis of the diffuse emission. North is up and East is to the left. See Section 3 for details.

reserved. The resulting effective exposure after data processing was 27 ks.

3. Imaging Analysis

Figure 1 shows broadband (0.5–7 keV) Chandra smoothed (left panel) and unsmoothed (right panel) images of J1818, with a high-energy cutoff of 7 keV because we are interested in searching for faint extended diffuse emission, and the particle background dominates this emission above ∼7 keV. The images are exposure-corrected using the CIAO task *fluximage* with a bin size of 1 pixel. The broadband image on the left is smoothed using a Gaussian function of radius 2 pixels. We applied *wavdetect* tool to the ACIS-S3 cleaned image and find an X-ray source with the center of the brightest pixel positioned at $\alpha_{J2000} = 18^h18^m00^s.23$ and $\delta_{J2000} = -16°07'52''.86$. The uncertainty of this position is dominated by the Chandra X-ray Observatory (CXO) absolute position uncertainty of $0''.8$ (at 90% confidence level).[5] The image also shows evidence of diffuse emission of size ∼15″ around the magnetar.

In order to model the extent and nature of this diffuse emission, we simulated a set of 100 observations of J1818 with the Chandra Ray Tracer (ChaRT[6]) and MARX[7] (ver. 5.3.2) software packages, based on the parameters of the Chandra observation and blackbody spectrum as determined from the spectral fits (see Section 4). The ChaRT output was then supplied to MARX to produce the simulated event files and point-spread function (PSF) images. Different values (0.25, 0.30, and 0.35) of the *AspectBlur* parameter (which accounts for the known uncertainty in the determination of the aspect solution) were used to search for an excess corresponding to the extended emission. We created broadband (0.5–7.0 keV) radial profiles up to 15″ by extracting net counts in circular annuli centered on the magnetar, with an annular background region extending from 30″–40″, and rebinned the data to obtain better statistical precision. Figure 2 (left panel) shows the surface brightness profiles for J1818 with the profiles generated using ChaRT/MARX for different blur values. The solid horizontal line in black represents the background level. The figure shows a clear deviation from the model PSF at radii $\gtrsim 1''.5$, and the presence of extended diffuse emission out to ∼10″, beyond which the emission becomes comparable to the background level.

The extended emission indicates the possibility of a very compact pulsar wind nebula (PWN) and/or a dust-scattering halo. Therefore, we further examined the morphology for any evidence of asymmetry, as would be expected from a PWN. For this, we divided the 15″ region around J1818 into four quadrants of eight equal annuli, as shown in Figure 1 (right panel). The quadrants, centered on the pulsar, are oriented to the north, east, south, and west. The corresponding radial profiles are shown in Figure 2 (right panel). The surface brightness of the four quadrants do not vary significantly and remains consistent within errors.

4. Spectral Analysis

The spectral analysis was performed with XSPEC (v12.10.1f). The contributions from background point sources were removed prior to the extraction of spectra. All of the spectra extracted were grouped by a minimum of 20 counts per bin and the errors were calculated at the 90% confidence level. We used the *tbabs* model (Wilms et al. 2000) to describe photoelectric absorption by interstellar medium.

The spectrum of J1818 was extracted from a $1''.5$ radius circular region centered on the source, which encompasses more than ∼90% of the encircled energy radius for a point source observed on-axis with Chandra[8] at 1.49 keV. The background was chosen from an annular ring of 3″–5″ centered on the source. As the magnetar was very bright at the time of outburst, we investigated the possibility of pileup using WebPIMMS (version 4.10) and *jdpileup* model of the Chandra spectral-fitting software Sherpa convolved with an absorbed BB model to fit the magnetar spectrum (see Section 4). The

[5] https://cxc.harvard.edu/cal/ASPECT/celmon/
[6] http://cxc.harvard.edu/ciao/PSFs/chart2/index.html
[7] http://space.mit.edu/CXC/MARX/
[8] http://cxc.harvard.edu/proposer/POG/html/chap6.html

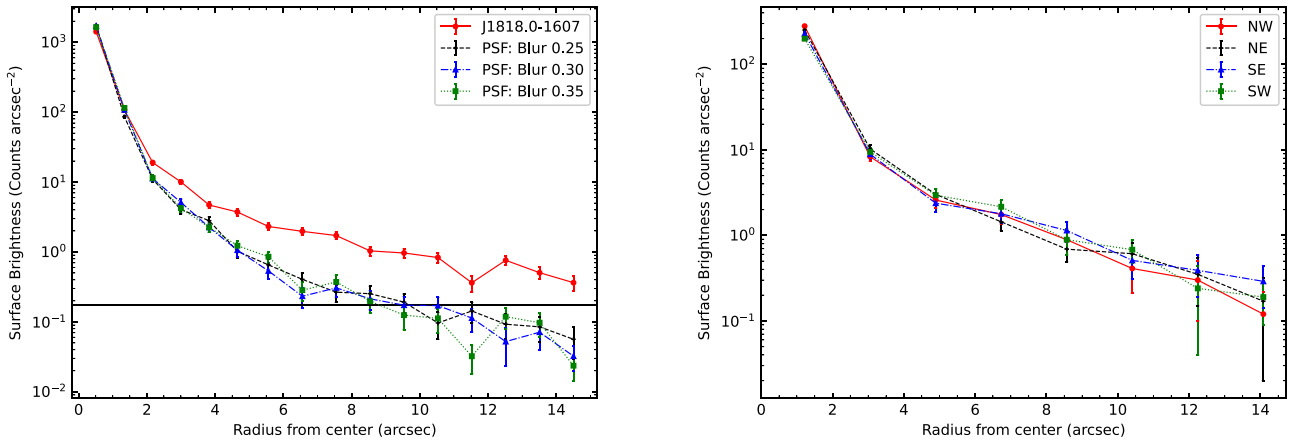

Figure 2. Left panel: surface brightness profiles of J1818 for different blur values. The black horizontal line represents the mean background level. Right panel:radial profiles for the four quadrants shown in Figure 1 (right): northwest (NW), northeast (NE), southwest (SW), and southeast (SE). See Section 3 for details.

WebPIMMS and Sherpa gave a pileup fraction of 24% and 35%, respectively.

The magnetar spectrum was fit with different models leaving all parameters to vary and included a pileup model (Davis 2001) as implemented in XSPEC. For the pileup component, only the grade-migration parameter (α) and the fraction of events in the source extraction region within the piled-up central portion of the PSF (*psffrac*) were allowed to vary. The pileup component improved the spectral fits quality and shape of the residuals substantially. A BB model yielded a good fit with hydrogen column density $N_H = 1.1^{+0.1}_{-0.1}\times10^{23}$ cm^{-2}, temperature $kT = 1.2 \pm 0.1$ keV, and unabsorbed flux $F_{BB} = 1.9^{+0.4}_{-0.3}\times10^{-11}$ erg cm^{-2} s^{-1}, as summarized in Table 1. When a PL model was used (χ^2_ν/dof $= 1.075/199$), the best-fit values were $N_H = 1.8^{+0.7}_{-0.5} \times 10^{23}$ cm^{-2} and photon index $\Gamma = 2.2 \pm 0.3$ with an unabsorbed flux $F_{\rm PL} = 4.5^{+1.0}_{-0.8}\times10^{-11}$ erg cm^{-2} s^{-1}. Although the PL model gave comparable fit statistics as the BB model, we obtained a flux exceeding the source flux at the time of outburst (see Esposito et al. 2020), likely due to high pileup. As there is also little PL contribution below 7 keV, we conclude that a single absorbed BB provides an adequate model to the source spectrum. The spectral fits were explored with different background regions and we found no significant differences in the spectral parameters. The addition of a second component was statistically not required. The best-fit BB spectrum is shown in Figure 3.

We determined the physical properties of the diffuse emission (see Figure 1) by selecting an annular ring of 3″–10″ region and a background of 30″–40″ radius centered on J1818. The extended emission has a total of 532 ± 25 background subtracted counts in the 1–10 keV range. An absorbed PL model provided a good fit with $N_H = 1.3^{+0.4}_{-0.3} \times 10^{23}$ cm^{-2}, $\Gamma = 2.0 \pm 0.5$, and an unabsorbed flux of $1.6^{+3.1}_{-1.0} \times 10^{-12}$ ergs cm^{-2} s^{-1}, as shown in Table 1.

Table 1
Spectral Fits to J1818 and Diffuse Emission

Parameter	BB	Diffuse Emission
N_H (cm^{-2})	$(1.1 \pm 0.1) \times 10^{23}$	$1.3^{+0.4}_{-0.3} \times 10^{23}$
Γ		2.0 ± 0.5
kT (keV)	1.2 ± 0.1	
$F_{\rm PL}$[a]		$1.6^{+3.1}_{-1.0}\times 10^{-12}$
$F_{\rm BB}$[a]	$1.9^{+0.4}_{-0.3}\times10^{-11}$	
χ^2_ν/dof	1.109/199	0.996/30
$L_{\rm X}$[b]	$9.6^{+2.0}_{-1.5} \times 10^{34}$	$8.1^{+0.2}_{-0.1} \times 10^{33}$

Note. Galactic absorption is modeled with *tbabs* in XSPEC using the abundances from Wilms et al. (2000). Errors are at 90% confidence level.
[a] Unabsorbed flux in units of erg cm^{-2} s^{-1}.
[b] X-ray luminosity (1–10 keV) in units of erg s^{-1} assuming isotropic emission at a distance of 6.5 kpc.

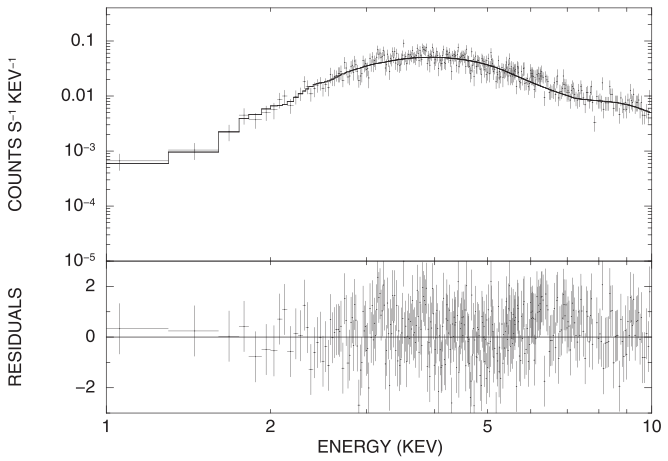

Figure 3. X-ray spectrum of Swift J1818 described by an absorbed blackbody model. The lower panel shows residuals in units of sigmas with error bars of size one.

5. Discussion and Conclusion

In this section, we discuss the analysis of Chandra observations of the newly discovered magnetar Swift J1818.0–1607 and associated compact extended emission, and explore its environment. The distance to the magnetar is estimated to be in the range of 4.8–8.1 kpc based on the Cordes–Lazio Galactic free electron density (NE2001; Cordes & Lazio 2002) and YMW2016 (Yao et al. 2017) models. We adopt an average distance of 6.5 kpc and introduce a scaling factor $d_{6.5} = d/6.5$ kpc to account for the distance uncertainty.

J1818 is the fifth magnetar to show radio emission and detected simultaneously in X-rays. It is also among the youngest magnetars in the Galaxy with an inferred characteristic age ∼470 yr (Hu et al. 2020). If the true age of J1818 is comparable to its characteristic age, we expect a young supernova remnant (SNR) surrounding the magnetar. The

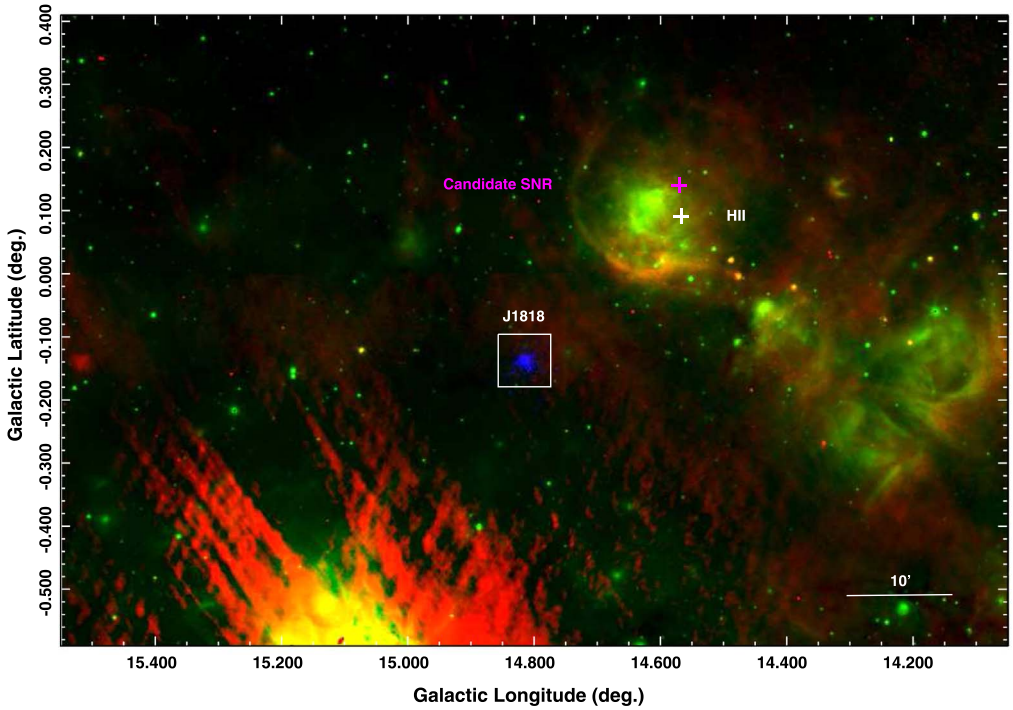

Figure 4. Multiwavelength image of the environment of J1818 with the MAGPIS 20 cm radio in red, MIPSGAL 24 μm infrared in green, and 0.5–7 keV Chandra image in blue. The images have been smoothed using a Gaussian function of radius 3 pixels. To the northwest of the magnetar lies an H II region overlapping with a candidate SNR, marked by magenta and white crosses, respectively. The centers of H II region and candidate SNR are marked by magenta and white crosses, respectively. The extremely bright source to the southeast is M17 (Messier 17). North is up and East is to the left. See Section 5 for details.

detection of any associated SNR shell will also help constrain the pulsar's true age because the characteristic age is unreliable, largely due to the implicit assumptions that all pulsars are born spinning very fast and spinning down under a constant braking index of 3. Therefore, we investigate the environment of J1818 by constructing a composite color image using the radio (red), infrared (green), and X-ray (blue) data, as shown in Figure 4. The radio image was obtained from the Multi-Array Galactic Plane Imaging Survey (MAGPIS[9]) at a wavelength of 20 cm (Helfand et al. 2006) and the infrared image from the survey of the inner Galactic plane using Spitzer's Multiband Imaging Photometer at a wavelength of 24 μm (MIPSGAL;[10] Carey et al. 2009). The infrared image shows that the magnetar lies in a complex region of the Galactic plane with several foreground or background sources, appearing in green.

To the northwest of the magnetar lies an H II region, G014.576+0.091 as identified in the WISE catalog[11], at $l = 14.467$, $b = 0.091$ and has a size of $\sim$425″. The near and far distance estimates to the H II region are 3.7 and 12.8 kpc (Table 6 of Anderson et al. 2014). We notice a nearly complete shell-like structure showing 20 cm continuum emission (in red) overlapping with this H II region. The 24 μm emission (in green) is also seen from the shell, but not inside as has been observed for H II regions. However, there are no cataloged SNRs around this position (Green 2019; Ferrand & Safi-Harb 2012 [12]). Therefore we speculate that this shell may be a possible candidate SNR at $l = 14.57$, $b = 0.14$, with a size of $\sim$11′. The position of J1818 is roughly 20′ from the candidate SNR's center. If we assume that J1818 was born at the center of this candidate SNR, and further assume an SNR age of $\sim$5–10 kyr (which is typical for SNRs in the Sedov phase), the magnetar would need a projected velocity of $\sim$3600–7300 km s^{-1} to reach its current location at a distance of 6.5 kpc. This estimate would be even higher if the SNR candidate were younger, making the association very unlikely. Proper motion measurements of J1818 and high-resolution radio observations are required to investigate any possible association, as well as confirm the nature and extent of the shell.

The Chandra spectrum of J1818 is best described by a BB model with $kT = 1.2 \pm 0.1$ keV and an unabsorbed flux of $1.9^{+0.4}_{-0.3} \times 10^{-11}$ ergs cm^{-2} s^{-1}. Assuming isotropic emission, the magnetar's X-ray luminosity is $L_X = 9.6^{+2.0}_{-1.5} \times 10^{34}\ d^2_{6.5}$ erg s^{-1}, implying an efficiency $\eta_X = L_X/\dot{E} \sim 0.13\ d^2_{6.5}$ in the 1–10 keV energy range. The neutron star's emitting radius inferred from the BB fit is 0.6 ± 0.1 km, which is slightly different from those reported by Esposito et al. (2020) and Hu et al. (2020). This can be attributed to Chandra's high imaging resolution, which allows us to disentangle the diffuse emission from the point source, as opposed to XMM-Newton or NICER. In the twisted magnetosphere model (Thompson et al. 2002), the thermal emission of magnetars is thought to originate from heating within the star due to the decay of the strong internal magnetic field. Twists in the magnetosphere suggest external heating to the surface. Twisted magnetic fields allow for the development of electric fields, accelerating particles off the surface resulting in a Comptonized BB-like spectrum (Beloborodov 2009). These particles can return to the surface, heating it through particle bombardment. For internal heating, it is simple heat diffusion toward the surface from the hotter core. Comparing the results obtained for J1818 with those of

[9] http://third.ucllnl.org/gps/
[10] http://mipsgal.ipac.caltech.edu
[11] http://astro.phys.wvu.edu/wise/
[12] http://snrcat.physics.umanitoba.ca

magnetars and high-B pulsars, its X-ray properties are similar to those seen in transient magnetars. Following outbursts, transient magnetars typically have high kT (>0.7 keV) compared to their quiescent BB temperatures of ≈0.4 keV (Coti-Zelati et al. 2017). It is also worth mentioning that J1818 has the highest spin-down luminosity (7.2×10^{35} erg s^{-1}) among the magnetars, followed by the radio magnetar 1E 1547.0–5408 with $\dot{E} = 2.1 \times 10^{35}$ erg s^{-1}. However, the inferred X-ray efficiency of J1818 is more in line with those of the high-B pulsars showing magnetar-like bursts with $L_X/\dot{E} \ll 1$. This, and the relatively high $\dot{E}$, imply that J1818 could be at least partly powered by rotation, similar to the rotation-powered pulsars.

The imaging analysis resolved a compact diffuse emission of $\geqslant 10''$ radius around J1818, with $N_H = 1.3^{+0.4}_{-0.3} \times 10^{23}$ cm^{-2}, hard $\Gamma = 2.0 \pm 0.5$, unabsorbed flux of $1.6^{+3.1}_{-1.0} \times 10^{-12}$ erg cm^{-2} s^{-1}, and a luminosity of $8.1^{-0.1}_{+0.2} \times 10^{33}\ d^2_{6.5}$ erg s^{-1} in the 1–10 keV band. The heavy absorption toward this region, combined with the brightening of the magnetar and its location in a crowded region of the Galactic plane, should cause scattering of point-source radiation by dust along the line of sight, forming a dust-scattering halo. Such halos have been observed around high-B pulsars, or magnetars (during an outburst), with index ranging from ∼2 to 5 as reported by several authors (e.g., Gotthelf et al. 2020; Tiengo et al. 2010; Younes et al. 2012; Israel et al. 2016). A dust-scattering halo typically shows symmetric structures around the point source and a softer spectrum than the illuminating source (i.e., the magnetar), as the scattering cross section of the dust particles scales as E^{-2} of the incident photon energies (Rivera-Ingraham & van Kerkwijk 2010). This is indeed the case here, where the diffuse emission seems fairly symmetric from the radial profile analysis and its spectrum marginally softer than J1818 (see Section 4). The magnetar spectrum below 10 keV is fit with a hotter BB temperature (Table 1) and a hard X-ray tail with $\Gamma = 0.0 \pm 1.3$ in the 1–20 keV band 3 days post outburst (Esposito et al. 2020). Both of these components are very hard and can result in a halo with a flatter spectrum (although softer than the source) as seen here with Chandra. Hence, it is likely that the diffuse emission around J1818 is dominated by a dust-scattering halo associated with the magnetar burst. Esposito et al. (2020) had also reported diffuse emission at radial distances of 50″–110″ from J1818, which could be the halo that was brighter at the time of XMM-Newton observations. As the Chandra observation was taken 21 days post outburst, it is possible that the halo has already become dimmer and smaller in size.

X-ray PWNe, with $\Gamma = 1$–2.5, have been observed around young ($\tau_c \sim 0.6$–30 kyr) rotation-powered pulsars (RPPs) with spin-down power $\dot{E}$ ranging from $\sim 10^{33}$–10^{38} erg s^{-1} (Kargaltsev & Pavlov 2008; Kargaltsev et al. 2013). J1818's young inferred age and relatively high $\dot{E}$ with respect to magnetars imply that it could power a compact PWN. The position of J1818 was observed previously with Chandra (ObsID: 8160, 2.7 ks exposure) in 2008 and XMM-Newton (ObsID: 0800910101, 60 ks exposure) in 2018. However, no point source or nebula emission was detected in these observations. It is possible that a faint nebula could be associated with J1818, but not detected in previous observations given the lack of sensitivity to such compact diffuse emission combined with heavy absorption. We can estimate an upper limit on the flux of a possible PWN undetected in previous Chandra observation (see Esposito et al. 2020 for XMM-Newton data) for the same extraction regions as in Section 4 with the ciao tool *srcflux*. We assume an $N_H = 1.3 \times 10^{23}$ cm^{-2} and a $\Gamma = 2$, as is typical of PWNe. The 3σ upper limit on the unabsorbed model flux is $\sim 2.3 \times 10^{-13}$ erg cm^{-2} s^{-1}, corresponding to a luminosity of $\sim 1.2 \times 10^{33}\ d^2_{6.5}$ erg s^{-1} and efficiency $\sim 0.002\ d^2_{6.5}$. This efficiency falls within the expected range of $\sim 10^{-6}$–10^{-1} observed in young pulsars with PWNe (Kargaltsev & Pavlov 2008) and is comparable to that of the high-B pulsar J1119–6127, which showed a magnetar-like burst in 2016. However, it is lower than what is typically observed in magnetars (see Table 1 of Safi-Harb 2013), suggesting that J1818 behaves more like a high-B rotation-powered pulsar than a magnetar. Interestingly, J1119–6127 also hosts a compact (∼10″ in radius) nebula with a quiescent luminosity of $\sim 1.9 \times 10^{32}$ erg s^{-1} (Safi-Harb & Kumar 2008; Blumer et al. 2017). The nebula was first detected in a 60 ks Chandra observation (Gonzalez & Safi-Harb 2003) and could not be resolved with XMM-Newton. Hence, deep Chandra observations of the magnetar in quiescence are necessary to investigate the nature of this extended emission and to search for the existence of any possible compact wind nebula.

To conclude, the sensitivity and resolution offered by Chandra allowed us to study the recently discovered magnetar Swift J1818.0–1607 and resolve compact faint emission surrounding it. Our study points to J1818 being a transient source showing properties intermediate between high-B pulsars and magnetars, and to the diffuse emission being dominated by a dust-scattering halo. Future deep Chandra observations of the source in quiescence will confirm the nature of this extended emission and place further constraints on any underlying compact wind nebula powered by the rotational energy loss of the pulsar.

The authors thank Chandra science team for making this DDT observation possible, Loren D. Anderson for useful discussions and providing the high-resolution MAGPIS and SPITZER images, and the anonymous referee for helpful comments that helped improve the manuscript. Support for this work was provided by the NASA grant DD0-21116X. S.S.H. acknowledges support by the Natural Sciences and Engineering Research Council of Canada and the Canadian Space Agency.

ORCID iDs

Harsha Blumer https://orcid.org/0000-0003-4046-884X
Samar Safi-Harb https://orcid.org/0000-0001-6189-7665

References

Anderson, L. D., Bania, T. M., Balser, D. D., et al. 2014, ApJS, 212, 1
Archibald, R. F., Kaspi, V. M., Tendulkar, S. P., & Scholz, P. 2016, ApJL, 829, L21
Beloborodov, A. M. 2009, ApJ, 703, 1044
Blumer, H., Safi-Harb, S., & McLaughlin, M. A. 2017, ApJL, 850, L18
Carey, S. J., Noriega-Crespo, A., Mizuno, D. R., et al. 2009, PASP, 121, 76
Champion, D., Desvignes, G., Jankowski, F., et al. 2020, ATel, 13559, 1
Cordes, J. M., & Lazio, T. J. W. 2002, arXiv e-prints, astro-ph/0207156
Coti-Zelati, F., Rea, N., Turolla, R., et al. 2017, MNRAS, 471, 1819
Davis, J. E. 2001, ApJ, 562, 575
Enoto, T., Sakamoto, T., Younes, G., et al. 2020, ATel, 13551, 1
Esposito, P., Rea, N., Borghese, A., et al. 2020, ApJL, 896, L30
Evans, P. A., Gropp, J. D., Kennea, J. A., et al. 2020, GCN, 27373, 1
Ferrand, G., & Safi-Harb, S. 2012, AdSpR, 49, 1313
Gavriil, F. P., Gonzalez, M. E., Gotthelf, E. V., et al. 2008, Sci, 319, 1802

Gonzalez, M. E., & Safi-Harb, S. 2003, ApJL, 591, L143
Gotthelf, E. V., Safi-Harb, S., Straal, S., & Gelfand, J. 2020, arXiv:2009.06616
Göğüş, E., Lin, L., Kaneko, Y., et al. 2016, ApJL, 829, L25
Green, D. A. 2019, JApA, 40, 36
Helfand, D. J., Becker, R. H., White, R. L., Fallon, A., & Tuttle, S. 2006, AJ, 131, 2525
Hu, C.-P., Begicarslan, B., Guver, T., et al. 2020, ApJ, 902, 1
Israel, G. L., Esposito, P., Rea, N., et al. 2016, MNRAS, 547, 3448
Kargaltsev, O., & Pavlov, G. G. 2008, in AIP Conf. Proc. 983, 40 Years of Pulsars: Millisecond Pulsars, Magnetars and More, ed. C. Bassa et al. (Melville, NY: AIP), 171
Kargaltsev, O., Rangelov, B., & Pavlov, G. G. 2013, arXiv e-prints, astro-ph/1305.2552
Karuppusamy, R., Desvignes, G., Kramer, M., et al. 2020, ATel, 13553, 1
Kaspi, V. M., & Beloborodov, A. M. 2017, ARA&A, 55, 261
Kumar, H. S., & Safi-Harb, S. 2008, ApJL, 678, L43
Rea, N., Borghese, A., Esposito, P., et al. 2016, ApJL, 828, L13
Rea, N., Esposito, P., Turolla, R., et al. 2010, Sci, 330, 944
Rivera-Ingraham, A., & van Kerkwijk, M. H. 2010, ApJ, 710, 797
Safi-Harb, S. 2013, in Proc. IAU Symp. 291, Neutron Stars and Pulsars: Challenges and Opportunities after 80 years, ed. J. van (Cambridge: Cambridge Univ. Press), 251
Safi-Harb, S., & Kumar, H. S. 2008, ApJ, 684, 532
Thompson, C., Lyutikov, M., & Kulkarni, S. R. 2002, ApJ, 574, 332
Tiengo, A., Vianello, G., Esposito, P., et al. 2010, ApJ, 710, 227
Wilms, J., Allen, A., & McCray, R. 2000, ApJ, 542, 914
Yao, J. M., Manchester, R. N., & Wang, N. 2017, ApJ, 835, 29
Younes, G., Kouveliotou, C., Kargaltsev, O., et al. 2016, ApJ, 824, 138